

# Electrical resistivity and thermopower of $(\text{La}_{1-x}\text{Sr}_x)\text{MnO}_3$ and $(\text{La}_{1-x}\text{Sr}_x)\text{CoO}_3$ at elevated temperatures

T. Ohtani \*, K. Kuroda, K. Matsugami, D. Katoh

Laboratory for Solid State Chemistry, Okayama University of Science, Ridai-cho 1-1, Okayama 700-0005, Japan

## Abstract

Electrical resistivity and Seebeck ( $S$ ) measurements were performed on  $(\text{La}_{1-x}\text{Sr}_x)\text{MnO}_3$  ( $0.02 \leq x \leq 0.50$ ) and  $(\text{La}_{1-x}\text{Sr}_x)\text{CoO}_3$  ( $0 \leq x \leq 0.15$ ) in air up to 1073 K.  $(\text{La}_{1-x}\text{Sr}_x)\text{MnO}_3$  ( $x \leq 0.35$ ) showed a metal-to-semiconductor transition; the transition temperature almost linearly increased from  $\sim 250$  to  $\sim 390$  K with increasing Sr content. The semiconductor phase above the transition temperature showed negative values of  $S$ .  $(\text{La}_{1-x}\text{Sr}_x)\text{CoO}_3$  ( $0 \leq x \leq 0.10$ ) showed a semiconductor-to-metal transition at  $\sim 500$  K. Dominant carriers were holes for the samples of  $x \geq 0.02$  above room temperature.  $\text{LaCoO}_3$  showed large negative values of  $S$  below ca. 400 K, indicative of the electron conduction in the semiconductor phase. © 2000 Elsevier Science Ltd. All rights reserved.

**Keywords:** Electrical properties;  $\text{La}_{1-x}\text{Sr}_x\text{MO}_3$  ( $M = \text{Mn, Co}$ ); Perovskite; Powders-solid state reaction; Transition metal oxides;

## 1. Introduction

Perovskite oxides have been extensively studied for the past four decades because of their interesting electrical and magnetic properties.<sup>1,2</sup>  $(\text{La}_{1-x}\text{Sr}_x)\text{MnO}_3$  is a promising candidate for the cathode of solid oxide fuel cells.<sup>3–5</sup>  $(\text{La}_{1-x}\text{Sr}_x)\text{MnO}_3$  is known to show a metal-to-semiconductor transition near the ferromagnetic Curie temperature in the range of  $x$  between  $\sim 0.1$  and  $\sim 0.45$ .<sup>1</sup> The sample of  $x = \sim 0.17$  shows a huge negative magnetoresistance called colossal magnetoresistance.<sup>6,7</sup> There are several reports on high-temperature electrical resistivity<sup>3,8–10</sup> and high-temperature Seebeck measurements<sup>10–12</sup> of  $\text{LaMnO}_3$  and the Sr-doped system.

$(\text{La}_{1-x}\text{Sr}_x)\text{CoO}_3$  has been also investigated for use in various high-temperature electrochemical devices such as solid oxide fuel cells<sup>13</sup> and oxygen permeation membranes.  $(\text{La}_{1-x}\text{Sr}_x)\text{CoO}_3$  shows a semiconductor-to-metal transition at ca. 500 K.<sup>1</sup> Recently it was found that this transition is accompanied by a spin state change from the intermediate-spin ( $t_{2g}^5 e_g^1$  configuration) to the high-spin ( $t_{2g}^4 e_g^2$  configuration) state.<sup>14–16</sup> High-temperature electrical resistivity and Seebeck measurements for  $(\text{La}_{1-x}\text{Sr}_x)\text{CoO}_3$  were performed by some investigators.<sup>17–20</sup>

So far, however, there are few reports on systematic high-temperature electrical measurements on both  $(\text{La}_{1-x}\text{Sr}_x)\text{MnO}_3$  and  $(\text{La}_{1-x}\text{Sr}_x)\text{CoO}_3$  systems. In the present work, we performed electrical resistivity ( $\rho$ ) and Seebeck ( $S$ ) measurements on the systems of  $(\text{La}_{1-x}\text{Sr}_x)\text{MnO}_3$  ( $0.02 \leq x \leq 0.50$ ) and  $(\text{La}_{1-x}\text{Sr}_x)\text{CoO}_3$  ( $0 \leq x \leq 0.15$ ) in the wide temperature range up to 1073 K.

## 2. Experiments

Samples of  $(\text{La}_{1-x}\text{Sr}_x)\text{MnO}_3$  ( $0.02 \leq x \leq 0.50$ ) and  $(\text{La}_{1-x}\text{Sr}_x)\text{CoO}_3$  ( $0 \leq x \leq 0.10$ ) were prepared as follows. Desired ratios of the mixture of  $\text{La}_2\text{O}_3$ ,  $\text{SrCO}_3$  and Mn (or Co) metal powder were pelletized and were heated at 1200°C for 7 days in air. After grinding, the products were pressed into a pellet under a pressure of 1800 kg/cm<sup>2</sup>. The pellets were heated again at the same temperature for 7 days in air, and then were slowly cooled to room temperature. Obtained specimens were identified by powder X-ray diffraction (XRD) method using an X-ray diffractometer (Rigaku:RAD-B) with  $\text{CuK}\alpha$  radiation.

High-temperature electrical resistivity ( $\rho$ ) measurements were performed on sintered pellets by d.c. four-probe method up to 1073 K in air. High-temperature Seebeck ( $S$ ) measurements were carried out on sintered pellets by keeping a temperature gradient of  $\sim 1$  K/mm up to 1073 K in air. Schematic experimental setup for Seebeck

\* Corresponding author.

measurements is illustrated in Fig. 1. A sintered pellet of the sample with a dimension of  $10 \times 5.0 \text{ mm}^2$  was sandwiched between two baked pyrophyllite plates. Temperature was measured by a thermocouple (chromel–alumel) attached at the center of the sample. A thermal gradient along a bar of the sample was measured by a differential thermocouple (chromel–alumel), and a thermal e.m.f. was measured through Au leads. Au leads and thermocouples are tightly attached to the sample. The experimental setup for high-temperature  $\rho$  measurements was similar to that for  $S$  measurements.

Resistivity measurements below room temperature were performed by an ordinary d.c. four probe method using Au paste. Low-temperature  $S$  measurements were carried out by similar way as adopted for high-temperature measurements, using Au paste. Temperature was measured with Au + 0.07 at.%Fe vs. chromel thermocouples in both low-temperature  $\rho$  and  $S$  measurements.

### 3. Results and discussion

#### 3.1. $(\text{La}_{1-x}\text{Sr}_x)\text{MnO}_3$

XRD patterns of  $(\text{La}_{1-x}\text{Sr}_x)\text{MnO}_3$  showed a pseudocubic perovskite-type structure. The patterns of samples with  $x \leq 0.35$  were similar to that of  $\text{LaMnO}_{3.09}$ , which was identified to have a  $\text{LaAlO}_3$  type structure by Takeda et al.<sup>9</sup> Samples with  $x \geq 0.40$  showed the patterns similar to that of  $\text{LaMnO}_{3.04}$  having a  $\text{GdFeO}_3$  type structure.<sup>9</sup>

Fig. 2(a) shows temperature variations of  $\rho$  of  $(\text{La}_{1-x}\text{Sr}_x)\text{MnO}_3$  ( $0.02 \leq x \leq 0.30$ ) observed on cooling. The curve for each sample showed a cusp at 300–400 K. The cusp would correspond to the ferromagnetic transition temperature.<sup>1</sup> Temperature variations were changed from metallic to semiconductive at the cusp temperature. The transition temperature will be referred to as  $T_t$ . Temperature variations of  $\rho$  were reversible below and above  $T_t$  in all samples, suggesting that the phase transition is not of the first order.  $T_t$  almost linearly

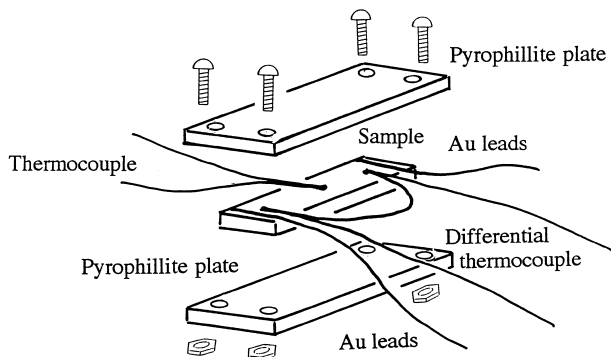


Fig. 1. Schematic experimental setup for Seebeck measurements at high temperatures.

increased from  $\sim 250$  to  $\sim 390$  K with increasing  $x$ . The value of  $\rho$  as well as the energy gap above  $T_t$  decreases continuously as  $x$  increases, suggesting that holes are introduced in the  $e_g$  orbital band by the substitution of  $\text{Sr}^{2+}$  for  $\text{La}^{3+}$ . The present observations are similar to those reported by Tokura et al., who carried out  $\rho$  measurements below 500 K.<sup>6</sup>

Fig. 2(b) shows temperature variations of  $\rho$  of  $(\text{La}_{1-x}\text{Sr}_x)\text{MnO}_3$  ( $0.35 \leq x \leq 0.50$ ) observed in cooling measurements. Temperature dependences of  $\rho$  for  $0.35 \leq x \leq 0.45$  were substantially similar to those for  $x \leq 0.30$ , while the cusp became to be broadened. It is noted that  $(\text{La}_{0.5}\text{Sr}_{0.5})\text{MnO}_3$  showed the different temperature variation of  $\rho$  as compared with other samples, i.e. the sample showed a change from metal to semiconductor at  $\sim 300$  K on cooling. We observed quite identical behaviors in samples with  $0.55 \leq x \leq 0.65$ . It is known that the ferromagnetism disappears around  $x = 0.50$ .<sup>1</sup> The different temperature dependence of  $\rho$  for  $x = 0.50$  would be related to the disappearance of the Curie transition. Kikuchi et al. observed the entire disappearance of ferromagnetism in  $(\text{La}_{1-x}\text{Sr}_x)\text{MnO}_3$  with  $x > 0.6$ , and observed a sudden increase of  $\rho$  around

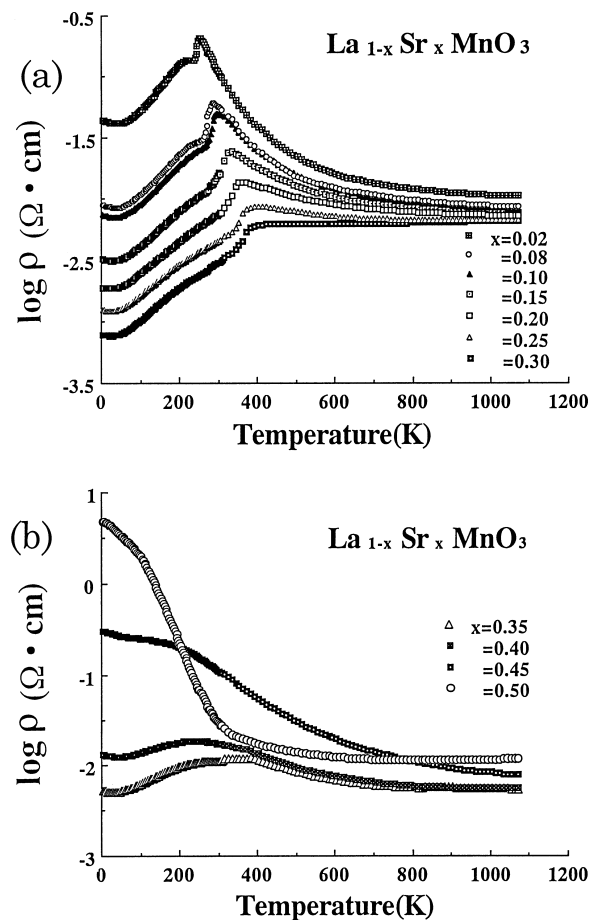


Fig. 2. Temperature variations of the resistivity ( $\rho$ ) of  $(\text{La}_{1-x}\text{Sr}_x)\text{MnO}_3$  for  $0.02 \leq x \leq 0.30$  (a), and for  $0.35 \leq x \leq 0.50$  (b).

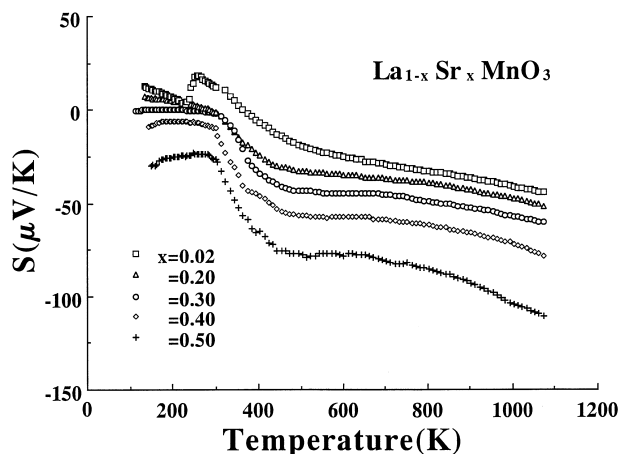


Fig. 3. Temperature variations of Seebeck coefficients ( $S$ ) of  $(\text{La}_{1-x}\text{Sr}_x)\text{MnO}_3$  ( $0.02 \leq x \leq 0.50$ ).

250 K on cooling for  $0.50 \leq x \leq 1.0$ .<sup>21</sup> Their observations are compatible with the present results for  $(\text{La}_{0.5}\text{Sr}_{0.5})\text{MnO}_3$ . These results suggest that the transition near 300 K has no relation to the long-range magnetic ordering.

Fig. 3 shows temperature variations of Seebeck coefficients ( $S$ ) of  $(\text{La}_{1-x}\text{Sr}_x)\text{MnO}_3$  measured on cooling from 1073 to  $\sim 100$  K. For simplicity, results of only five samples of  $x = 0.02, 0.20, 0.30, 0.40$ , and  $0.50$  are shown in the figure. The values of  $S$  of  $(\text{La}_{0.98}\text{Sr}_{0.02})\text{MnO}_3$  were negative at high temperatures, indicating the electron conduction. The values gradually increased with lowering temperature, and then changed sign from minus to plus at ca. 350 K. Below  $T_i$ , the value of  $S$  of this sample was ca.  $+10 \mu\text{V/K}$ , indicative of the metallic conduction with holes as dominant carriers. The sample showed a small drop at  $\sim 250$  K on cooling, which corresponds to  $T_i$  observed in  $\rho$  measurements. For  $0.20 \leq x \leq 0.50$ , temperature dependences of  $S$  are similar to each other, while the values of  $S$  decrease with increasing  $x$ . The  $S$ - $T$  curves of these samples showed a kink at 300–400 K, which temperature seems to be almost invariable with  $x$ , and is lower than  $T_i$  observed in  $\rho$  measurements. The values of  $S$  of these samples were negative above  $\sim 300$  K, suggesting that the dominant carriers are electrons in the simple conduction model. Asamitsu et al. reported that the sign of  $S$  changes from plus to minus at the transition temperature for  $x = \sim 0.2$ .<sup>22</sup> In the region of  $0.2 \leq x \leq 0.3$ , they observed the charge carrier change from electronlike to holelike with the increase of spin-polarization by lowering temperature or by applying magnetic field, which was interpreted in terms of a change of electronic structure relating to the orbital degree of freedom of the  $e_g$  carriers.<sup>22</sup> The negative  $S$  was also observed in  $\text{LaMnO}_{3+\delta}$  ( $\delta \geq 0.07$ ) at high temperatures by Töpfer and Goodenough,<sup>10</sup> and in  $(\text{La}_{1-x}\text{Sr}_x)\text{MnO}_3$  ( $x = 0, 0.1$ ) above  $\sim 400$  K by Raffaele et al.<sup>11</sup> Stevenson et al. observed negative  $S$  in a wide

temperature range above ca. 400 K in the system of  $(\text{La}_{1-x}\text{Ca}_x)\text{MnO}_3$  ( $x = 0, 0.2, 0.4, 0.6$ ).<sup>12</sup> High-temperature thermopower of  $\text{LaMnO}_3$  and  $(\text{La}_{1-x}\text{A}_x)\text{MnO}_3$  ( $A = \text{Ca}, \text{Sr}$ ) was theoretically discussed by Marsh and Parris, who employed a model for small polaron conduction which occurs through the  $e_g$  transition-metal manifold.<sup>23</sup> Their calculation predicts that the doped systems show the negative  $S$  at elevated temperatures, and that the value of  $S$  decreases (the absolute value of  $S$  increases) with increasing dopant concentration,  $x$ . Present results are in good agreement with their calculation. Temperature variation of  $S$  for  $(\text{La}_{0.5}\text{Sr}_{0.5})\text{MnO}_3$ , which shows no magnetic ordering, was substantially identical with that of other samples with  $x < 0.5$ . Samples of  $0.55 \leq x \leq 0.65$  also showed similar temperature variations of  $S$ . The similarity of  $S$ - $T$  curves in all samples indicate that the magnetic ordering does not play an important role in thermoelectric effects, and in the phase transition.

### 3.2. $(\text{La}_{1-x}\text{Sr}_x)\text{CoO}_3$

Samples of  $(\text{La}_{1-x}\text{Sr}_x)\text{CoO}_3$  ( $0 \leq x \leq 0.15$ ) were identified to have a rhombohedrally distorted perovskite structure, which is in accordance with the earlier observations.<sup>19,24</sup> XRD patterns for  $(\text{La}_{1-x}\text{Sr}_x)\text{CoO}_3$  are shown in Fig. 4. The patterns are identical with JCPDS data.<sup>25</sup> Lattice parameters of  $\text{LaCoO}_3$  were  $a = 5.443 \text{ \AA}$ , and  $c = 13.08 \text{ \AA}$  in the hexagonal system. Both parameters increased with increasing Sr content.

Fig. 5 shows temperature dependences of  $\rho$  for  $(\text{La}_{1-x}\text{Sr}_x)\text{CoO}_3$  ( $0 \leq x \leq 0.15$ ) observed in cooling measurements.  $\text{LaCoO}_3$  showed a metal-to-semiconductor transition at 500–600 K. The energy gap in the semiconductor phase of  $\text{LaCoO}_3$  was observed to be 0.29 eV, which value is rather compatible with the earlier observation.<sup>18</sup> Samples of  $0.02 \leq x \leq 0.10$  showed the behaviors similar to that of  $\text{LaCoO}_3$ , with the energy gap in the semiconductor phase decreasing as  $x$  increases. In the sample of  $x = 0.15$  the transition was scarcely observed. The present results are well consistent with the earlier results obtained by Bhide et al.<sup>18</sup> and Kobayashi et al.<sup>20</sup>

Fig. 6 shows temperature variations of  $S$  for  $(\text{La}_{1-x}\text{Sr}_x)\text{CoO}_3$  ( $0 \leq x \leq 0.15$ ) observed in cooling measurements. The values of  $S$  of the Sr-substituted samples were positive in measured temperature range, indicative of hole conduction. For samples of  $0.02 \leq x \leq 0.05$ , the value of  $S$  was  $+20$ – $30 \mu\text{V/K}$  at 1073 K, followed by gradual increase with decreasing temperature. The values of  $S$  began to sharply increase at  $\sim 500$  K, corresponding to the transition observed in  $\rho$  measurements. The values of  $S$  reached to  $+300$ – $600 \mu\text{V/K}$  at 300 K. Relatively low values of  $S$  above the transition temperature indicate the metallic conduction, and the high values below the transition temperature the semiconductive conduction, which are well consistent with the  $\rho$  data. The decreasing tendency of  $S$  with increasing

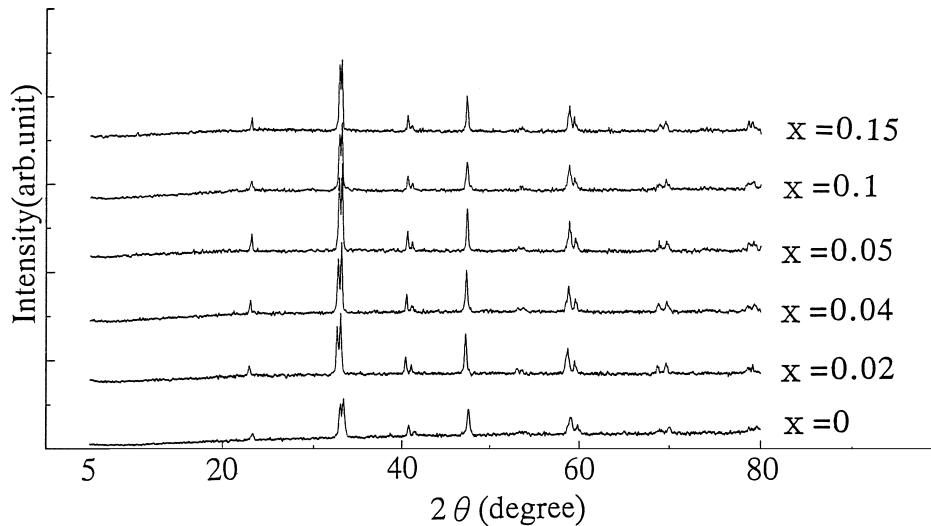


Fig. 4. X-ray diffraction patterns for  $(\text{La}_{1-x}\text{Sr}_x)\text{CoO}_3$  ( $0 \leq x \leq 0.15$ ) observed with  $\text{CuK}_\alpha$  radiation.

$x$  shows that the hole density increases with increasing  $x$ , which is well explained by that holes are introduced by the  $\text{Sr}^{2+}$  substitution for  $\text{La}^{3+}$ . Samples of  $x \geq 0.10$  showed low values of  $S$  in the wide temperature range, indicative of metallic conductivity as observed in the  $\rho$  measurements. These behaviors of  $S$  are quite compatible with earlier data for Sr-substituted samples obtained by Bhide et al.<sup>18</sup>

The most striking observation is that  $\text{LaCoO}_3$  showed a change of sign of  $S$  from plus to minus at ca. 400 K, suggesting that the dominant carriers are electrons in the semiconductor phase. As far as we know, there is no report on the negative  $S$  for  $\text{LaCoO}_3$ . In order to elucidate the origin of the electron conduction, we prepared  $\text{LaCoO}_3$  under different oxygen partial pressures using  $\text{O}_2$  gas (99.9% in purity) and Ar gas (99.999% in purity) in the same heat treatments as adopted for the preparation

in air. It is easily expected that the sample prepared under  $\text{O}_2$  gas contains more amount of oxygen atoms as compared with the sample prepared under Ar gas. Temperature variations of  $\rho$  of the samples prepared under both  $\text{O}_2$  and Ar atmosphere showed the behaviors quite identical with that of the sample prepared in air. Fig. 7 shows  $S$  as a function of  $T^{-1}$  for  $\text{LaCoO}_3$  prepared under the different atmospheres.  $S$  measurements were carried out on heating from 110 to 1073 K. For the sample prepared under  $\text{O}_2$  gas, the  $S$ - $T$  curve is concave upward exhibiting a minimum ( $S \cong -100 \mu\text{V/K}$ ) near 250 K, and at 100 K the value of  $S$  reaches to as high as  $+900 \mu\text{V/K}$ . For the sample obtained in air, the value of  $S$  decreases with lowering temperature, showing a minimum ( $S \cong -300 \mu\text{V/K}$ ) near 140 K. In the case of preparation under Ar atmosphere the sample showed the lowest values of  $S$  among three samples below room

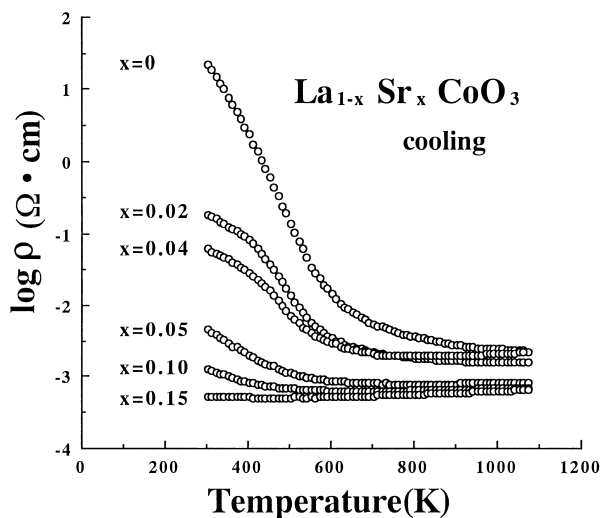


Fig. 5. Temperature variations of the resistivity ( $\rho$ ) for  $(\text{La}_{1-x}\text{Sr}_x)\text{CoO}_3$  ( $0 \leq x \leq 0.15$ ) observed in cooling measurements.

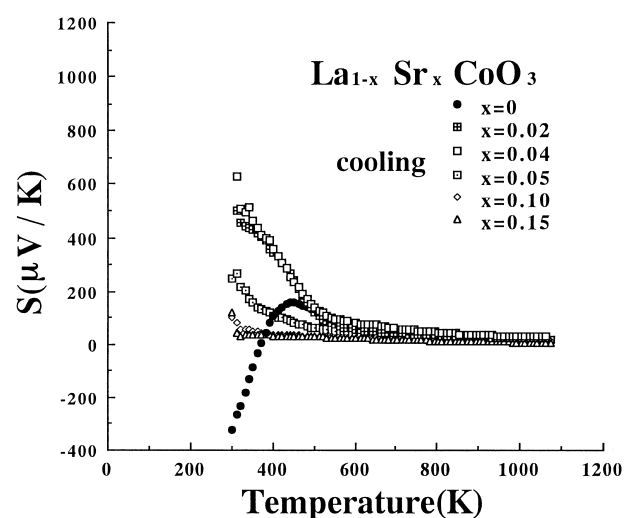


Fig. 6. Temperature variations of Seebeck coefficient ( $S$ ) for  $(\text{La}_{1-x}\text{Sr}_x)\text{CoO}_3$  ( $0 \leq x \leq 0.15$ ) observed in cooling measurements.

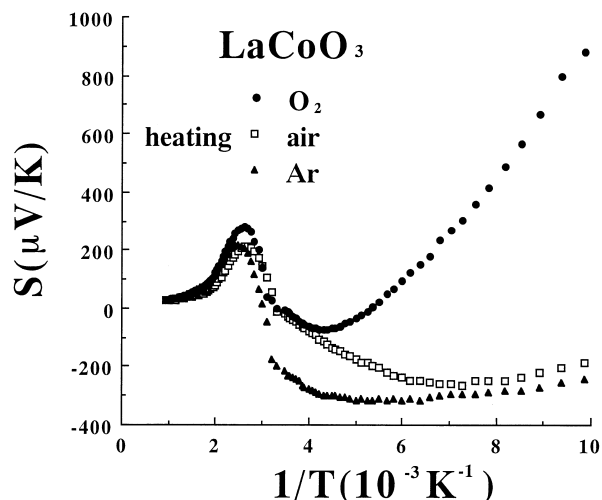


Fig. 7. Temperature variations of Seebeck coefficients ( $S$ ) for  $\text{LaCoO}_3$ , which was obtained by heating at  $1200^\circ\text{C}$  under  $\text{O}_2$ , air, or Ar atmosphere.

temperature. The decreasing tendency of  $S$  with decreasing oxygen content suggests that electrons are introduced for the charge compensation in the oxygen-deficient samples.

Our preliminary Hall measurements also showed the electron conduction for  $\text{LaCoO}_3$  at room temperature. Band calculations predicted a gapless semiconductor or a half-metallic character for  $\text{LaCoO}_3$ .<sup>14,26</sup> This prediction, however, is not consistent with the semiconductive behaviors in  $\text{LaCoO}_3$  observed in the present  $\rho$  and  $S$  measurements. Saitoh et al. observed in their photoemission and X-ray-absorption spectroscopy measurements that  $\text{LaCoO}_3$  is a charge-transfer-type insulator having the band gap with considerable  $p$ - $p$  character due to the strong hybridization.<sup>15</sup> We suppose that the low-temperature phase of  $\text{LaCoO}_3$  is a donor-type semiconductor. Photoemission and X-ray-absorption spectroscopy measurements<sup>27</sup> and Hall measurements<sup>20</sup> showed that the band structure of  $(\text{La}_{1-x}\text{Sr}_x)\text{CoO}_3$  cannot be explained by the rigid-band-semiconductor model. Present observation of the different carrier type between  $\text{LaCoO}_3$  and the Sr-substituted samples would support these earlier observations.<sup>20,27</sup>

#### 4. Summary

Perovskite oxides of  $(\text{La}_{1-x}\text{Sr}_x)\text{MnO}_3$  ( $0.02 \leq x \leq 0.50$ ) and  $(\text{La}_{1-x}\text{Sr}_x)\text{CoO}_3$  ( $0 \leq x \leq 0.15$ ) were prepared by heating the desired ratios of the mixture of  $\text{La}_2\text{O}_3$ ,  $\text{SrCO}_3$  and Mn (or Co) at  $1200^\circ\text{C}$  in air. Electrical resistivity ( $\rho$ ) and Seebeck ( $S$ ) measurements were performed on sintered pellets up to  $1073$  K in air.  $(\text{La}_{1-x}\text{Sr}_x)\text{MnO}_3$  ( $x \leq 0.35$ ) showed the transition from a metal (low-temperature phase) to a semiconductor (high-temperature phase). The transition temperature

almost linearly increased from  $\sim 250$  to  $\sim 390$  K with increasing Sr content. The semiconductor phase showed negative values of  $S$ , which is compatible with the calculation results presented by Marsh and Parris.<sup>23</sup>  $(\text{La}_{1-x}\text{Sr}_x)\text{CoO}_3$  ( $0 \leq x \leq 0.10$ ) showed the transition from a semiconductor (low-temperature phase) to a metal (high-temperature phase) at ca.  $500$  K.  $S$  measurements showed that the dominant carriers were holes for samples of  $x \geq 0.02$  in measured temperature range ( $300$ – $1073$  K). The hole density increased with increasing  $x$ , which was well explained by that holes were introduced by the substitution of  $\text{Sr}^{2+}$  for  $\text{La}^{3+}$ .  $\text{LaCoO}_3$  showed large negative values of  $S$  below ca.  $400$  K, indicating that the low-temperature phase of  $\text{LaCoO}_3$  is a donor-type semiconductor.

#### Acknowledgements

This work was partially supported by a Special Grant for Cooperative Research administered by the Japan Private School Promotion Foundation.

#### References

- Goodenough, J. B., *Metallic oxides*. In *Progress in Solid State Chemistry*, vol. 5, ed. H. Reiss. Pergamon, Oxford, 1971, pp. 145–399.
- Rao, C. N. R. and Gopalakrishnan, J., *New Direction in Solid State Chemistry*, 2nd ed. Cambridge University Press, Cambridge, 1997.
- Hammouche, A., Schouler, E. J. L. and Henault, M., Electrical and thermal properties of Sr-doped lanthanum manganites. *Solid State Ionics*, 1988, **28**(30), 1205–1207.
- Kamata, H., Hosaka, A., Mizusaki, J. and Tagawa, H., High temperature electrocatalytic properties of the SOFC air electrode  $\text{La}_{0.8}\text{Sr}_{0.2}\text{MnO}_3/\text{YSZ}$ . *Solid State Ionics*, 1998, **106**, 237–245.
- Mizusaki, J., Mori, N., Takai, H., Yonemura, Y., Minamiue, H., Tagawa, H., Dokiya, M., Inaba, H., Naraya, K., Sazamoto, T. and Hashimoto, T., Oxygen nonstoichiometry and defect equilibrium in the perovskite-type oxides  $\text{La}_{1-x}\text{Sr}_x\text{MnO}_{3+\delta}$ . *Solid State Ionics*, 2000, **129**, 163–177.
- Tokura, Y., Urushibara, A., Moritomo, Y., Arima, T., Asamitsu, A., Kido, G. and Furukawa, N., Giant magnetotransport phenomena in filling-controlled kondo lattice system:  $\text{La}_{1-x}\text{Sr}_x\text{MnO}_3$ . *J. Phys. Soc. Japan*, 1994, **63**, 3931–3935.
- Mahesh, R., Mahendiran, R., Raychaudhuri, A. K. and Rao, C. N. R., Giant magnetoresistance in bulk samples of  $\text{La}_{1-x}\text{A}_x\text{MnO}_3$  (A = Sr or Ca). *J. Solid State Chem.*, 1995, **114**, 297–299.
- Jonker, G. H., Magnetic and semiconducting properties of perovskites containing manganese and cobalt. *J. Appl. Phys.*, 1966, **37**, 1424–1430.
- Takeda, Y., Nakai, S., Kojima, T., Kanno, R., Imanishi, N., Shen, G. Q., Yamamoto, O., Mori, M., Asakawa, C. and Abe, T., Phase relation in the system  $(\text{La}_{1-x}\text{A}_x)_{1-y}\text{MnO}_{3+z}$  (A = Sr and Ca). *Material Research Bulletin*, 1991, **26**, 153–162.
- Töpfer, J. and Goodenough, J. B.,  $\text{LaMnO}_{3+\delta}$  revisited. *J. Solid State Chem.*, 1997, **130**, 117–128.
- Raffaella, R., Anderson, H. U., Sparlin, D. M. and Parris, P. E., Transport anomalies in the high-temperature hopping conductivity and thermopower of Sr-doped  $\text{La}(\text{Cr},\text{Mn})\text{O}_3$ . *Phys. Rev.*, 1991, **B43**, 7991–7999.

12. Stevenson, J. W., Nasrallah, M. M., Anderson, H. U. and Sparlin, D. M., Defect structure of  $Y_{1-y}Ca_yMnO_3$  and  $La_{1-y}Ca_yMnO_3$ . I. Electrical properties. *J. Solid State Chem.*, 1993, **102**, 175–184.
13. Kawada, T., Masuda, K., Suzuki, J., Kaimai, A., Kawamura, K., Nigara, Y., Mizusaki, J., Yugami, H., Arashi, H., Sakai, N. and Yakogawa, H., Oxygen isotope exchange with a dense  $La_{0.6}Sr_{0.4}CoO_{3-\delta}$  electrode on a  $Ce_{0.9}Ca_{0.1}O_{1.9}$  electrolyte. *Solid State Ionics*, 1999, **121**, 271–279.
14. Korotin, M. A., Ezhov, S. Yu, Solovyev, I. V., Anisimov, V. I., Khomskii, D. I. and Sawatzky, G. A., Intermediate-spin state and properties of  $LaCoO_3$ . *Phys. Rev.*, 1996, **B54**, 5309–5316.
15. Saitoh, T., Mizokawa, T., Fujimori, A., Abbate, M., Takeda, Y. and Takano, M., Electronic structure and temperature-induced paramagnetism in  $LaCoO_3$ . *Phys. Rev.*, 1997, **B55**, 4257–4266.
16. Asai, K., Yoneda, A., Yokokura, O., Tranquada, J. M., Shirane, G. and Kohn, K., Two spin-state transitions in  $LaCoO_3$ . *J. Phys. Soc. Japan*, 1998, **67**, 290–296.
17. Rao, C. N. R., Bhide, V. G. and Mott, N. F., Hopping conduction in  $La_{1-x}Sr_xCoO_3$  and  $Nd_{1-x}Sr_xCoO_3$ . *Phil. Mag.*, 1975, **32**, 1277–1282.
18. Bhide, V. G., Rajoria, D. S., Rao, C. N. R., Rama, Rao G. and Jadhao, V. G., Itinerant-electron ferromagnetism in  $La_{1-x}Sr_xCoO_3$ : a Mössbauer study. *Phys. Rev.*, 1975, **B12**, 2832–2843.
19. Mineshige, A., Kobune, M., Fujii, S., Ogumi, Z., Inaba, M., Yao, T. and Kikuchi, K., Metal-insulator transition and crystal structure of  $La_{1-x}Sr_xCoO_3$  as functions of Sr-content, temperature, and oxygen partial pressure. *J. Solid State Chem.*, 1999, **142**, 374–381.
20. Kobayashi, Y., Murata, S., Asai, K., Tranquada, J. M., Shirane, G. and Kohn, K., Magnetic and transport properties of  $LaCo_{1-x}Ni_xO_3$  — comparison with  $La_{1-x}Sr_xCoO_3$ . *J. Phys. Soc. Japan*, 1999, **68**, 1011–1017.
21. Kikuchi, K., Chiba, H., Kikuchi, M. and Syono, Y., Syntheses and magnetic properties of  $La_{1-x}Sr_xMnO_y$  ( $0.5 \leq x \leq 1.0$ ) perovskite. *J. Solid State Chem.*, 1999, **146**, 1–5.
22. Asamitsu, A., Moritomo, Y. and Tokura, Y., Thermoelectric effect in  $La_{1-x}Sr_xMnO_3$ . *Phys. Rev.*, 1996, **B53**, R2952–R2955.
23. Marsh, D. B. and Parris, P. E., High-temperature thermopower of  $LaMnO_3$  and related systems. *Phys. Rev.*, 1996, **B54**, 16602–16607.
24. Liu, J., He, L., Chen, G. and Su, W., A study on selected properties of  $La_{1-x}Sr_xCoO_3$  and its application in sealed  $CO_2$  lasers. *J. Mater. Sci.*, 1997, **32**, 203–206.
25. JCPDS File No. 25-1060; No. 28-1229.
26. Hamada, N., Sawada, H. and Terakura, K., Electronic band structures of  $LaMO_3$  ( $M = Ti, V, Cr, \dots, Ni, Cu$ ) in the local spin-density approximation. In *Spectroscopy of Mott Insulators and Correlated Metals*, ed. A. Fujimori and Y. Tokura. Springer, Berlin, 1995, pp. 95–105.
27. Saitoh, T., Mizokawa, T., Fujimori, A., Abbate, M., Takeda, Y. and Takano, M., Electronic structure and magnetic states in  $La_{1-x}Sr_xCoO_3$  studied by photoemission and x-ray-absorption spectroscopy. *Phys. Rev.*, 1997, **B56**, 1290–1295.